1	Copper intoxication in group B Streptococcus triggers transcriptional activation
2	of the <i>cop</i> operon that contributes to enhanced virulence during acute infection
3	Matthew J. Sullivan ^a , Kelvin G. K. Goh ^a , Dean Gosling ^{a,†} , Lahiru Katupitiya ^a , and Glen
4	C. Ulett ^{a #}
5	
6	^a School of Medical Sciences, and Menzies Health Institute Queensland, Griffith
7	University, Gold Coast, Queensland, Australia 4222.
8	[†] Current address: Pathology Queensland, Health Support Queensland, Department of
9	Health, Queensland Government, Southport, Queensland, Australia 4215.
10	
11	Article Type: Research article
12	Running Title: Copper stress in group B Streptococcus
13	Word count: 4960, 198 (abstract)
14	Display Items : 7 Figures, 2 Tables (plus 1 Supplementary Table, 1 Supplementary Fig)
15	Conflict Statement: All the authors do not have a commercial or other association that
16	might pose a competing financial interest in relation to the work described.
17	
18	# Correspondence and offprint requests: Professor Glen C. Ulett, School of Pharmacy
19	and Medical Science, and Menzies Health Institute Queensland, Griffith Health Centre,
20	Griffith University, Gold Coast, Queensland 4222, Email: g.ulett@griffith.edu.au, T: +61
21	7 56780765, F: +61 7 55632236

22 Abstract

23 Bacteria require Copper (Cu) as an essential trace element to support cell processes: 24 however, excess Cu can intoxicate bacteria. Here, we characterize the *cop* operon in 25 group B Streptococcus (GBS), and establish its role in evasion of Cu intoxication and 26 the response to Cu stress on virulence. Growth of GBS mutants deficient in either the 27 copA Cu exporter, or the copY repressor, were severely compromised in Cu-stress 28 conditions. GBS survival of Cu stress reflected a mechanism of CopY activation of the 29 CopA efflux system. However, neither mutant was attenuated for intracellular survival in 30 macrophages. Analysis of global transcriptional responses to Cu by RNA-sequencing 31 revealed a stress signature encompassing homeostasis of multiple metals. Genes 32 induced by Cu stress included putative metal transporters for manganese import, 33 whereas a system for iron export was repressed. In addition, *copA* promoted the ability 34 of GBS to colonize the blood, liver and spleen of mice following disseminated infection. 35 Together, these findings show that GBS *copA* mediates resistance to Cu intoxication, 36 via regulation by the Cu-sensing transcriptional repressor, copY. Cu stress responses in 37 GBS reflect a transcriptional signature that heightens virulence and represents an 38 important part of the bacteria's ability to survive in different environments. 39

40 Keywords: Metallobiology; group B *Streptococcus*; Metal ions; Copper efflux; Bacterial
41 pathogenesis

42 Introduction

43 Copper (Cu) is the most reactive of the biologically-relevant first-row d-block transition 44 metals. It can readily displace other metals, including Zinc (Zn), Nickel (Ni), Cobalt (Co), 45 Iron (Fe) and Manganese (Mn) from metalloproteins in which these are bound (1, 2). In 46 cells across all Kingdoms of life, Cu-dependent enzymes are pivotal to many essential 47 processes that underpin physiologic biochemical reactions, owing to its ability to redox 48 cycle between Cu(I) and Cu(II) states (3). When present in excess, however, Cu is 49 hazardous to cellular processes and macromolecules due to effects of localized free-50 radical damage (4). A key role for Cu in bacterial cell biology encompasses the host-51 pathogen interface where a balance between Cu usage and avoidance of Cu 52 intoxication resulting from host antimicrobial responses must be attained for bacteria to 53 survive, as reviewed elsewhere (5). At this interface, human immune cells can mobilize 54 Cu in a defence response to infection that culminates in exposure of intracellular 55 bacteria to antimicrobial levels of Cu that kill the invading pathogen (6-9). Thus, 56 bacterial responses to Cu stress and mechanisms of resistance to metal-ion intoxication 57 have emerged as important facets of bacterial disease pathogenesis (10). 58 59 There are several mechanisms that enable bacteria to tolerate excess extracellular Cu. 60 and these have been characterized in several pathogenic species. These mechanisms, 61 which represent survival strategies against Cu intoxication (10) typically involve Cu-62 transporting P-type ATPases, exemplified by CopA, which detoxify Cu by exporting it

from the bacterial cytosol (11-13). This mechanism has been described in gram-

negative and gram-positive bacteria, and among *Streptococcaceae* (14-16), including
pneumococci and *Streptococcus pyogenes* (17).

66

67 An opportunistic streptococcal pathogen of humans and animals for which resistance to 68 excess extracellular Cu has not been described is Streptococcus agalactiae, also known 69 as group B streptococcus (GBS). This organism, unlike other Streptococcaceae, is 70 associated with a comparatively broad host-range that encompasses humans, cattle 71 and fish (18). In humans, GBS is a major cause of invasive infection in infants <3 72 months of age (19), and causes a more diverse range of disease aetiologies compared 73 to other streptococci, including meningitis, pneumonia, skin and soft-tissue infections, 74 sepsis, arthritis, osteomyelitis, urinary tract infection, and endocarditis (19). GBS has a 75 several virulence factors that enable survival in cytotoxic environments, such as acid 76 stress, oxidative stress, and during host colonization, as reviewed elsewhere (20). 77 Cellular tolerance to Cu stress and mechanisms of responding to and surviving Cu 78 intoxication have not been defined in GBS. 79 80 In this study, we characterise a system that enables Cu efflux in GBS, encompassing a

81 *copA*-homologue, which we show mediates control of Cu efflux in the bacteria. We

82 show this system affects survival, growth and virulence of GBS in the mammalian host.

83

84 Results

85 Transcriptomic profiling of GBS responses to extracellular Cu

86 To dissect the global response of GBS to extracellular Cu stress we performed RNA

87 sequencing (RNASeq) to define the complete primary transcriptional response to Cu.

88 RNASeq analysis of mid-log phase cells of GBS strain 874391 exposed to 0.5 mM Cu

89 (a sub-inhibitory level; below) compared to non-exposed controls revealed a surprisingly

90 modest Cu-responsive transcriptome. The response comprised 18 transcriptional

91 responses, defined as significant based on $-2 \le FC \ge 2$ (FDR < 0.05, *n*=4 biological

92 replicates), of 11 up-regulated transcripts and 7 down-regulated transcripts (Figure 1,

Table 1). The most significantly up-regulated were homologues of the *copY-copA-copZ*

94 gene cluster (3.6-4.0-fold), which encode the putative CopY (Cu-binding transcriptional

95 repressor), CopA (P-type ATPase Cu-efflux system) and CopZ (Cu-chaperone) proteins.

96 To validate the expression levels of selected targets identified in RNASeq, we targeted

97 *pcl1*, *hvgA* and *copY* in qRT-PCR assays, confirming near-identical fold-change values

to RNASeq analyses (Figure 1B). The products of *copY*, *copA* and *copZ* in GBS (Figure

99 2A) are moderately conserved compared to other Lactobacillales, including *S. mutans*,

100 S. thermophilus, S. pyogenes, S. pneumoniae, and Enterococcus (Figure 2B, ranked by

101 CopA similarity) for which a homologous Cu management system is defined (9, 13-15).

Together, these findings provide transcriptional and comparative insights that support aproposed model of Cu efflux in GBS (Figure 2C).

104

105 In addition to *cop YAZ*, GBS up-regulated putative metal transporters for Mn import

106 (*mtsABC*, *mntH2*), and down-regulated an iron (Fe) export system (*fetAB*; Figure 1,

Table 1). In addition, we detected significant down-regulation of *pcl1*, that encodes a
putative membrane protein, and the gene for hypervirulence-associated factor, *hvgA*.

109

110 Roles of copA and copY in Cu-resistance in GBS

111 To provide molecular functional characterization of two of the major elements of the Cu-112 responsive transcriptome in GBS, we targeted *copA* and *copY* by generating isogenic 113 deletion mutants and performing comparative growth assays with the WT. In a nutrient-114 rich medium (Todd Hewitt Broth; THB) supplemented with increasing amounts of Cu, 115 we detected no significant attenuation effect of high Cu levels (up to 1.5 mM) on the 116 growth of WT GBS; the lag phases, growth rates, and final biomass yields were 117 equivalent for the WT exposed to different levels of Cu (Figure 3). In contrast, $\triangle copA$ 118 GBS exhibited a major attenuation for growth in conditions of Cu stress ≥ 1 mM. 119 Deletion of copY. encoding a putative Cu-dependent repressor of copA, had no effect 120 on the growth rate or lag phase in THB supplement with Cu (Figure 3). Taken together, 121 these data establish that *copA* confers cellular resistance to Cu stress in GBS in a 122 manner that supports bacterial growth in nutritive conditions.

123

124 Temporal- and Concentration-Dependent Bactericidal effects of Cu towards GBS

To more precisely define the toxicity effects of Cu towards GBS, we performed time-kill curves using $1-5 \times 10^6$ CFU/mL exposed to Cu concentrations ranging between 50μ M and 1 mM. We used a minimal Chemically-Defined Medium (CDM) in the context of prior studies of antibacterial activity in minimal media (21, 22), that antibacterial activity in such assays can be strongly dependent on the culture media (23, 24), and to minimize cell-

130 protective effects that can result from some buffering agents, such as glutathione (15). 131 We found potent killing effects that depended on both concentration and time with ≥ 0.5 132 mM Cu significantly killing WT GBS after 6h of exposure (Figure 4, WT); after 24h, there 133 was a ~230-fold reduction in CFU/mL at 0.5 mM Cu (0 mM Cu = $5.6 \text{ Log}_{10} \text{ CFU/mL}$, 0.5 134 mM CFU/mL = 3.2 Log_{10} CFU/mL), and no viable GBS remained in cultures exposure to 135 1 mM Cu. The $\triangle copA$ strain was significantly more susceptible to Cu toxicity compared 136 to the WT; Cu levels above ≥ 0.5 mM significantly reduced the number of viable $\triangle copA$ 137 GBS beginning as early as 1h exposure (Figure 4, $\triangle copA$); the degree of bacterial killing 138 was dramatic at the 24h timepoint for ≥ 0.5 mM Cu (Figure 4). Complementation of the 139 copA mutation in trans restored the phenotype to WT levels of growth (Supplementary 140 Figure S1). Interestingly, at the 6h timepoint, high Cu (≥ 0.5 mM) did not affect viability 141 of $\triangle cop Y GBS$, compared to the WT strain (Figure 4, $\triangle cop Y$), a hyper-resistance 142 phenotype that was not apparent at the 24 h timepoint. Together, these findings are 143 consistent with a role for CopA in resisting Cu stress and CopY as a repressor of Cu 144 resistance.

145

*Regulation of Cu efflux by CopY, and accumulation of metals during Cu stress*We next sought to identify regulatory mechanisms controlling the Cu-response in GBS at the genetic level. The capacity of Cu stress to induce expression of *copA* for Cu export was examined by analyzing *copA* expression by qRTPCR in GBS exposed to Cu Cu concentrations ranging from 0.25-1.5 mM Cu in THB. GBS significantly upregulated *copA* in response to Cu (3.7-fold – 14.2-fold) in a manner that was titratable with the Cu concentration (Figure 5A). To ascertain the role of CopY as a putative Cu-responsive

153 repressor of *copA* expression in GBS, we quantified *copA* mRNA transcripts in the 154 $\Delta cop Y$ mutant exposed to 0.5 mM Cu. This level of Cu was carefully chosen as sub-155 inhibitory to enable comparisons independent of metabolic state and therefore limiting 156 any potential bias from possible discordant Cu stress between WT and mutants with 157 varied resistance phenotypes. Deletion of *copY* impacted final biomass yield of cultures 158 compared to WT (Figure 5B), and resulted in severe de-regulation of *copA* expression, 159 causing a ~207±45-fold increase of *copA* transcripts in the *copY* background (Figure 160 5C). Thus, *copA* responds transcriptionally to extracellular Cu, and GBS *copY* functions 161 to repress *copA* in the absence of Cu.

162

163 To examine the impact of *copA* and *copY* mutations on accumulation of Cu within the 164 cell we used the equivalent conditions per RNASeg and gPCR assays, exposing GBS 165 to 0.5 mM Cu in THB and measuring total Cu content of cells compared to non-exposed 166 controls. Inductively coupled optical emission spectroscopy (ICP-OES) demonstrated 167 that standard THB contained 0.2±0.08 µM Cu, reflecting trace amounts in the medium. 168 In the absence of supplemental Cu, WT GBS limited intracellular Cu content such that 169 only 0.8±0.1 µg Cu. g dry weight⁻¹ were detected in cultures grown in THB. However, 170 exposure of WT GBS to 0.5 mM Cu resulted in a dramatic increase in intracellular Cu to 171 31.9±3.1 µg Cu, g dry weight⁻¹ (Figure 5D). Strikingly, $\triangle cop Y$ GBS exhibited significantly less cellular Cu upon exposure to Cu (6.7±0.4 µg Cu, g drv weight⁻¹), consistent with the 172 173 observation that transcription of the Cu-exporter CopA is significantly elevated in this 174 mutant. In addition, we noted massive accumulation of cellular Cu in the $\triangle copA$ strain 175 (109.6±1.9 µg Cu. g dry weight⁻¹), confirming a Cu-efflux role for *copA*. Interestingly, we

- 176 noted no changes in other metals, including Zn, Mn and Fe (data not shown) in WT
- 177 versus $\triangle copA$ GBS, consistent with a report in S. pneumoniae (14).
- 178

179 Role of CopA in macrophage killing of GBS

180 To examine whether the CopA Cu efflux system in GBS supports survival of the bacteria

181 in phagocytes we performed antibiotic protection assays with murine macrophages and

182 human monocyte-derived macrophage-like cells. Macrophages were infected with WT

- 183 or *△copA* GBS for 1h, and antibiotics were added to kill extracellular bacteria. Viable
- 184 intracellular GBS were quantified at 1h post-antibiotic addition, and at 24h and 48h.

185 These assays demonstrated significant reduction in the numbers of viable GBS over the

time course (24 to 48h) in both human and murine macrophages; however, there were

187 no significant differences detected between the numbers of WT and $\triangle copA$ GBS

188 recovered from macrophages at any time point (Figure 6). Thus, under these conditions,

189 *copA* does not contribute to the intracellular survival of GBS in macrophages.

190

191 GBS CopA contributes to virulence in vivo

192 To examine the contribution of Cu efflux to GBS virulence, we used a murine model of

disseminated infection (25). In mice challenged with 10⁷ GBS, we detected significantly

194 fewer $\triangle copA$ mutant in the liver (median of 3.5 vs 4.2 log₁₀ CFU.g tissue⁻¹; P= 0.005),

spleen (median of 3.8 vs 4.1 \log_{10} CFU.g tissue⁻¹ P= 0.013) and blood (median of 1.4 vs

196 1.9 \log_{10} CFU.mL⁻¹; P= 0.044) compared to the WT at 24h post-inoculation (Figure 7).

197 No differences were observed between counts of the WT and $\triangle copA$ mutant in the

198 brain, heart, lungs, or kidneys (data not shown). These data support a modest but

- 199 statistically significant role for cellular management of Cu via *copA* in supporting
- 200 disseminated infection in vivo.

201

202 Materials and Methods

203 Bacterial strains, plasmids and growth conditions

- 204 GBS, *E. coli* and plasmids used are listed in Table 2. GBS was routinely grown in Todd-
- Hewitt Broth (THB) or on TH agar (1.5% w/v). *E. coli* was grown in Lysogeny Broth (LB)
- 206 or on LB agar. Media were supplemented with antibiotics (spectinomycin (Sp)
- 207 100 μ g/mL; chloramphenicol (Cm) 10 μ g/mL), as indicated. Growth assays used 200 μ L
- 208 culture volumes in 96-well plates (Greneir) sealed using Breathe-Easy® membranes
- 209 (Sigma Aldrich) and measured attenuance (*D*, at 600nm) using a ClarioSTAR
- 210 multimode plate reader (BMG Labtech) in Well Scan mode using a 3mm 5x5 scan
- 211 matrix with 5 flashes per scan point and path length correction of 5.88mm, with agitation
- at 300rpm and recordings taken every 30min. Media for growth assays were THB and a
- 213 modified Chemically-Defined Medium (CDM) (26) (with 1g/L glucose, 0.11g/L pyruvate
- and 50µg/L L-cysteine), supplemented with Cu (supplied as CuSO₄) as indicated. For
- attenuance baseline correction, control wells without bacteria were included for Cu in
- 216 media alone.

217 DNA extraction and genetic modification of GBS

- 218 Plasmid DNA was isolated using miniprep kits (QIAGEN), with modifications for GBS as
- 219 described elsewhere (27). Deletions in *copA* (CHF17_00507 / CHF17_RS02570) and
- 220 copY(CHF17_00506 / CHF17_RS02565) were constructed by markerless allelic
- exchange using pHY304aad9 as described previously (28). Plasmids and primers are
- listed in Table 2 and Supplementary Table S1, respectively. Mutants were validated by
- 223 PCR using primers external to the mutation site and DNA sequencing.
- 224 **RNA extraction, qRTPCR**

225 For Cu exposure experiments, 1mL overnight THB cultures were back-diluted 1/100 in 226 100mL of THB (prewarmed at 37°C in 250mL Erlenmeyer flasks) supplemented with 227 0.25, 0.5, 1.0 or 1.5mM Cu. Cultures were grown shaking (200rpm) at 37°C; after 228 exactly 2.5h, 10-50mL volumes containing approximately 500 million mid-log bacteria 229 were harvested; RNA was preserved and isolated as described previously (29). RNA 230 guality was analysed by RNA LabChip using GX Touch (Perkin Elmer). RNA (1000ng) 231 was reverse-transcribed using Superscript IV according to manufacturer's instructions 232 (Life Technologies) and cDNA was diluted 1:50 in water prior to gPCR. Primers 233 (Supplementary Table S1) were designed using Primer3 Plus (30, 31) to quantify 234 transcripts using Universal SYBR Green Supermix (Bio-Rad) using a Quantstudio 6 235 Flex (Applied Biosystems) system in accordance with MIQE guidelines (32). Standard 236 curves were generated using five-point serial dilutions of genomic DNA (5-fold) from WT 237 GBS 874391 (33). Expression ratios were calculated using C_T values and primer 238 efficiencies as described elsewhere (34) using *dnaN*, encoding DNA polymerase III β-239 subunit as housekeeper.

240 Whole bacterial cell metal content determination

Metal content in cells was determined as described (35) with minor modifications.
Cultures were prepared essentially as described for *RNA extraction, qRTPCR* with the
following modifications; THB medium was supplemented with 0.5 mM CuSO₄ or not
supplemented (Ctrl), and following exposure for 2.5h, bacteria were harvested by
centrifugation at 4122 x g at 4°C. Cell pellets were washed 3 times in PBS + 5mM
EDTA to remove extracellular metals, followed by 3 washes in PBS. Pelleted cells were
dried overnight at 80°C and resuspended in 1mL of 32.5% nitric acid and incubated at

248	95°C for 1h. The metal ion containing supernatant was collected by centrifugation
249	(14,000 x g, 30min) and diluted to a final concentration of 3.25% nitric acid for metal
250	content determination using inductively coupled plasma optical emission spectroscopy
251	(ICP-OES). ICP-OES was carried out on an Agilent 720 ICP-OES with axial torch,
252	OneNeb concentric nebulizer and Agilent single pass glass cyclone spray chamber. The
253	power was 1.4kW with 0.75L/min nebulizer gas, 15L/min plasma gas and 1.5L/min
254	auxiliary gas flow. Cu was analyzed at 324.75nm, Zn at 213.85nm, Fe at 259.94nm and
255	Mn at 257.61nm with detection limits at <1.1ppm. The final quantity of each metal was
256	normalised using dry weight biomass of the cell pellet prior to nitric acid digestion,
257	expressed as μ g.g ⁻¹ dry weight. Baseline concentrations were determined to be 0.2 ±
258	0.08 μM Cu in THB medium, and 40 \pm 4 nM Cu in CDM medium from at least three
259	independent assays.

260 **RNA sequencing and bioinformatics**

261 Cultures were prepared as described above for RNA extraction, gRTPCR to compare 262 mid-log phase cells grown in THB + 0.5 mM Cu to THB without added Cu. RNase-free 263 DNase-treated RNA that passed Bioanalyzer 2100 (Agilent) analysis was used for RNA 264 sequencing (RNA-seq) using the Illumina NextSeq 500 platform. We used TruSeq 265 library generation kits (Illumina, San Diego, California). Library construction consisted of 266 random fragmentation of the poly(A) mRNA, followed by cDNA production using random 267 primers. The ends of the cDNA were repaired and A-tailed, and adaptors were ligated 268 for indexing (with up to 12 different barcodes per lane) during the sequencing runs. The 269 cDNA libraries were quantitated using qPCR in a Roche LightCycler 480 with the Kapa 270 Biosystems kit (Kapa Biosystems, Woburn, Massachusetts) prior to cluster generation.

Clusters were generated to vield approximately 725K–825K clusters/mm². Cluster 271 272 density and quality was determined during the run after the first base addition 273 parameters were assessed. We ran paired-end 2×75 -bp sequencing runs to align the 274 cDNA sequences to the reference genome. For data preprocessing and bioinformatics, 275 STAR (version 2.7.3a) was used to align the raw RNA sequencing fast reads to the 276 WT GBS 874391 reference genome (33). HTSeq-count, version 0.11.1, was used to 277 estimate transcript abundances (36). DESeq2 was then used to normalized and test for 278 differential expression and regulation. Genes that met certain criteria (i.e. fold change of 279 > ± 2.0 , g value (false discovery rate, FDR of <0.05) were accepted as significantly 280 altered (37). Raw and processed data were deposited in Gene Expression Omnibus 281 (accession no. GSE161127).

282 Mammalian cell culture

283 J774A.1 murine macrophages or U937 human monocyte-derived macrophages (MDMs) 284 were grown in RPMI and seeded (10⁵) into the wells of a 96-well tissue culture-treated 285 plate (Falcon) essentially as described elsewhere (38, 39), except that U937 MDMs 286 were differentiated by exposure to 30ng/mL phorbol 12-myristate 13-acetate (PMA) for 287 48h and cells subsequently rested in media without PMA for 72h to enhance 288 morphological and phenotypic markers of MDMs (40). A multiplicity of infection (MOI) of 289 100 bacteria: macrophage for 1h was used in RPMI without antibiotics. Non-adherent 290 bacteria were removed by five washes of 200µL PBS using a Well Wash Versa (Thermo 291 Scientific). RPMI containing 250U/mL penicillin, streptomycin (Gibco) and 50µg/mL 292 gentamicin (Sigma-Aldrich) were used for antibiotic protection assays to kill extracellular 293 bacteria as described previously by incubating for 1h at 37°C in 5% CO₂ (39). Samples

294	were processed after 1h	time zero), 24h or 48h after infection, monolayers w	/ere

- washed five times with 200µL PBS and lysed by brief exposure to 50µL of 2% trypsin
- and 0.02% Triton-X-100 (10min) prior to dilution with 150µL PBS and estimation of
- 297 CFU/mL by serial dilution and plate counts on agar. Relative CFU (rCFU) was
- 298 determined as described previously (41) as follows; rCFU= CFU.mL⁻¹ at 24h or 48h /
- 299 CFU.mL⁻¹ at time zero.

300 Animals and Ethics statement

- 301 Virulence was tested using a mouse model of disseminated infection based on
- intravenous challenge with 10^7 GBS (WT or \triangle copA) as described elsewhere (25). This
- 303 study was carried out in accordance with the guidelines of the Australian National
- 304 Health and Medical Research Council. The Griffith University Animal Ethics Committee
- 305 reviewed and approved all experimental protocols for animal usage according to the
- 306 guidelines of the National Health and Medical Research Council (approval:
- 307 MSC/01/18/AEC).

308 Statistical methods

- 309 All statistical analyses used GraphPad Prism V8 and are defined in respective Figure
- 310 Legends. Statistical significance was accepted at P values of ≤ 0.05 .
- 311

312 Discussion

313 Transcriptional and cellular responses of bacterial pathogens to metal ions including Cu 314 can influence host-pathogen interactions and thereby play a role in disease pathogenesis 315 (4). The role Cu homeostasis and detoxification in the biology of GBS have not hitherto 316 been characterized, and no reports of a Cu stress response in this important human and 317 animal pathogen are published. The principal finding of this study is the establishment 318 of a transcriptional and cellular connection between the response to Cu stress in GBS 319 and survival of the bacteria in conditions of Cu toxicity; this connection is mediated 320 through copA and controlled through copY, and enables the bacteria to resist killing via 321 Cu-mediated intoxication. Additionally, this study establishes that the connection 322 between Cu stress responses in GBS and bacterial survival promotes virulence in the 323 host during systemic, disseminated infection. The new insights into gene function in 324 GBS viewed through the lens of the Cu stress transcriptome, combined with the findings 325 of enhanced virulence elucidate molecular mechanisms that underpin GBS survival of 326 intoxicating conditions, including those likely to be encountered in the host.

327

The transcriptional remodelling that occurs in GBS in response to Cu stress, as defined in this study on a global level, comprises an intriguingly constrained subset of genes. These findings indicate a tightly controlled system of transcriptional responses to Cu in GBS. Interestingly, equivalent low numbers of target genes were identified in previous transcriptional analyses of other streptococci exposed to Cu stress (14-16). Our findings are consistent with these prior reports, and support the notion that these transcriptional responses function in housekeeping or homeostasis to set a low limit of Cu availability 335 in the cytoplasm (15). In GBS, copA is among the most strongly activated genes in the 336 transcriptional response to Cu stress, and the mutational analysis performed in this 337 study shows that *copA* is crucial for the bacteria to attain an essential Cu efflux response 338 during Cu stress. However, copA is only one of an assembly of genes engaged by GBS 339 during Cu stress and it is likely that other genes in the transcriptome contribute to Cu 340 detoxification via additional means. For example, we detected up-regulation of putative 341 metal transporters for Mn import (*mtsABC*, *mntH2*) along with concurrent downregulation of a system that encodes Fe export machinery (fetAB). These transcriptional 342 343 insights are interesting because they hint at additional stress response mechanisms that 344 occur during Cu stress in GBS, which extend beyond CopA and which need elucidation. 345 346 Transcription of metal ion-import and export genes, including those above-mentioned, is

347 typically controlled by metal-dependent regulatory proteins termed metalloregulators that 348 sense metal ion-bioavailability and work to maintain cellular metal homeostasis (42). In 349 our study, we detected no major changes in the expression of genes predicted to encode 350 metalloregulators, such as for transport of Mn (*mntR/mtsR*), Fe (*fur*), Zn (*adcR/sczA*) and 351 for the sensing of peroxide (*perR*) in GBS undergoing Cu stress (42, 43). It would be of 352 interest to elucidate whether such regulators undergo mis-metallation in GBS during Cu 353 stress, which might occur due to excess Cu likely outcompeting Mn and Fe for binding 354 sites in proteins; however, precisely if and how metalloregulators might respond to mis-355 metallation in GBS, if this actually occurs, will need to be elucidated by further study. 356

357 A previous study of S. pneumoniae reported a role for Mn in rescuing Cu toxicity in the 358 bacteria (14). The authors suggested that the mechanism of rescue related to 359 modulated expression of aerobic and anaerobic dNTP synthesis pathways, encoded by 360 *nrdF* and *nrdD*, respectively. If we consider that Mn rescues Cu-mediated inhibition of 361 dNTP synthesis, it is conceivable that Mn import may be linked to Cu stress in GBS. 362 Our transcriptional assays of WT GBS showed no response of *nrdD* expression to Cu 363 stress, consistent with the findings of Johnson *et al.* Nevertheless, we observed a highly 364 statistically significant, but modestly up-regulated response of the *nrdFIA* genes, 365 encoding the aerobic dNTP synthesis system (1.7-fold, FDR < 0.001), to Cu stress (data 366 not shown). The role of *nrdFIA* genes in the GBS response to Cu stress requires further 367 study, noting that NrdD encodes an iron-containing enzyme, whereas NrdF encodes a 368 Mn-dependent pathway, further hinting at a role for Mn in the GBS Cu stress response. 369

370 In S. pyogenes, Mn uptake is facilitated by mtsABC and is protective against peroxide 371 induced stress (43). Expression of *mtsABC* is up-regulated by Mn deficiency, and is 372 controlled by the MtsR regulator (43, 44). Mn import and Fe efflux are co-ordinated in 373 order to control the metalation of superoxide dismutase (43), which can use Mn or Fe at 374 its catalytic site in streptococci; noting that Mn uptake can be disrupted by Zn (35). 375 Recently, the Cu-sensing transcription factor Mac1p in *Candida* was shown to regulate 376 the cells response to Cu starvation by controlling Cu import, and control reactive oxygen 377 species homeostasis by repressing a Cu-containing superoxide dismutase and inducing 378 Mn-containing SOD3 (45). A system for the dual import of Mn and Fe in GBS is 379 encoded by *mntH* that is regulated by pH (46). In some strains of GBS, including the

hypervirulent ST17 lineage used in this study, two homologues of MntH exist, encoded by *mntH* and *mntH*2. This study demonstrates up-regulation of *mntH*2, but not *mntH*, in response to Cu, however the role of *mntH*2 is undefined in GBS. We also note that *mtsABC* and *mntH*2 are also up-regulated in concert with down-regulation of Fetransporting *fetAB* in response to Zn stress in GBS (47). Together, our data indicate that modulation of *mtsABC*, *mntH*2 and *fetAB* expression forms parts of a transcriptional signature of GBS to Zn stress.

387

388 It is notable that modulation of putative Mn (*mtsABC*) and Fe (*fetAB*) transporters, as 389 well as other proteins predicted to localise to the membrane (pcl1) or cell surface (hvqA) 390 in GBS in response to Cu stress takes place in the absence of altered cellular Mn or Fe 391 content. This leads us to suggest that examining the roles of targets identified in this 392 study in the context of Cu transport is needed in concert with other metals (*e.g.*, Mn). 393 Indeed, the 'dearth of information' on precisely how Cu is transported into bacterial cells 394 from the external environment represents a central mystery for Cu trafficking in bacteria 395 (48). Perhaps a system for Cu import is inversely regulated to a bona fide Cu export 396 system, in a fashion that parallels the identified acquisition and efflux systems for Zinc 397 described in streptococci (49).

398

Our assays of bacterial growth *in vitro* in conditions of Cu stress demonstrate that GBS
deficient in *copA* cannot grow as efficiently compared to the WT in conditions of elevated
extracellular Cu. The differences noted in GBS growth between nutritionally rich (THB)
and limited (CDM) media possibly reflect relative quantities of compounds that confer a

403 protective advantage for survival during Cu stress, such as glutathione (15) or other 404 thiol-containing amino acids that may interact with free Cu ions in solution. Glutathione is 405 not included in CDM as a separate chemical constituent but the quantities of methionine, cystine and cysteine are 30, 62.6 and 50 mg.L⁻¹. It is also possible that the 406 407 levels of Cu utilized in our assays are distinct to those in host niches. Importantly, 408 however, Cu exposure assays *in vitro* are almost certainly influenced by the compounds 409 present in the medium that likely affect levels of Cu that become inhibitory (15). Thus, 410 the Cu exposure assays used in this study are beneficial in establishing bona fide gene 411 function and revealing bacterial responses to a defined stress condition. 412 413 Our analysis of Cu content in GBS cells exposed to Cu stress in defined conditions 414 shows that GBS maintains low steady-state levels of cellular Cu, in the absence of 415 excess extracellular Cu. In supplying extracellular Cu in excess, we show the level of 416 cellular Cu content is increased. Our finding that copY functions to repress copA in the 417 absence of Cu is consistent with previous reports in other bacteria (50, 51). Disrupting 418 the genetic systems for Cu efflux in GBS, via mutation of the CopA exporter, or the 419 CopY regulator, reveals divergent phenotypes that stem from loss of export or 420 regulatory function, resulting in accumulation (copA) or reduction (copY) of cellular Cu. 421 These phenotypes will be of interest to dissect in terms of the role of CopY in GBS 422 biology in other models of infection and disease in the future. 423 424 Historically, studies have demonstrated increased Cu levels in the blood of humans

425 during bacterial infection (52, 53) but most insight into Cu-driven antimicrobial

426 responses is derived from *in vitro* studies of mammalian cells infected experimentally. In 427 macrophages, bioavailability of Cu correlates with antibacterial activities (54), and Cu 'hot 428 spot' formation mediates antimicrobial responses against intracellular bacteria (7). The 429 cellular consequences of Cu stress to GBS, which likely encounters such stress in the 430 host, remains undefined. Our findings based on *in vitro* infection macrophages showed 431 no attenuation of GBS devoid of CopA in survival in host cells, which was surprising 432 given the important role of Cu management in survival of other bacteria inside 433 macrophages (6), and epithelial cells (12). Notably, however, intracellular survival of 434 Salmonella deficient in cueO, which encodes an enzyme required for resistance to Cu 435 ions, was not impaired in murine macrophages in a previous study (55), leading the 436 authors to suggest multiple host factors are involved in clearance of the bacteria. Our 437 findings are consistent with these hypotheses. Other researchers have described the 438 limitations of *in vitro* tissue culture monolayer assays for determining intracellular survival 439 of bacteria in the context of Cu homeostasis (56).

440

441 Despite negative findings in macrophage monolayer assays in vitro, systemic infection of 442 mice exposed a connection between the ability of GBS to generate a Cu management 443 response via CopA and bacterial virulence *in vivo*. Here, *copA* was essential for GBS to 444 fully colonize and survive in the blood, as well as in other tissues. In demonstrating a 445 significant attenuation of GBS deficient in CopA to be fully virulent in mice, we suggest 446 that Cu toxicity may represent a form of stress experienced by the bacteria *in vivo* during 447 systemic infection. In other bacteria, including Pseudomonas aeruginosa and Listeria 448 monocytogenes, compromised Cu transport leads to attenuation for colonization in

449 various infection models (56, 57). Attenuation of GBS for colonization of the blood, liver 450 and spleen indicates that Cu management in the bacterial cell is essential not only for 451 efficient survival of the bacteria in the bloodstream but also for colonization of highly 452 immunologically active tissues; *i.e.*, Kupffer cells and splenic lymphocytes for innate and 453 adaptive immune responses, respectively. It would be of interest to analyze the effect of 454 Cu transport deficiency in GBS in other relevant models of infection, including in vaginal 455 colonization (58). Additional to defining the effects of metal homeostasis in GBS on the 456 nature of infection and disease caused by this organism, small-molecules probes might 457 hold promise for the identification of other molecular mechanisms of metal homeostasis 458 in GBS, as reported for Gram-positive bacteria (59).

459

In summary, this study shows that management of Cu export in GBS is essential for the bacteria to survive in environments of Cu stress. Cu intoxication in GBS generates a transcriptional signature that includes activation of the *cop* operon to confer bacterial survival and virulence in stressful environments. The exact role for Cu ions as an antibacterial response against GBS warrants further investigation.

466 Acknowledgements

- 467 We thank Michael Crowley and David Crossman of the Heflin Centre for Genomic
- 468 Science Core Laboratories, University of Alabama at Birmingham (Birmingham, AL) for
- 469 RNA sequencing. We also thank Ryan Stewart at the School of Environment Analytical
- 470 Chemistry Core Facility, Griffith University, for ICP-OES. This work was supported by a
- 471 Project Grant from the National Health and Medical Research Council (NHMRC)
- 472 Australia (APP1146820 to GCU).

473

474 References

- Waldron KJ, Rutherford JC, Ford D, Robinson NJ. 2009. Metalloproteins and
 metal sensing. Nature 460:823-30.
- 477 2. Irving H, Williams RJP. 1953. 637. The stability of transition-metal complexes.
- 478 Journal of the Chemical Society (Resumed) doi:10.1039/jr9530003192:3192-
- 479 3210.
- 480 3. Festa RA, Thiele DJ. 2011. Copper: an essential metal in biology. Curr Biol
 481 21:R877-83.
- 482 4. Ladomersky E, Petris MJ. 2015. Copper tolerance and virulence in bacteria.

483 Metallomics 7:957-64.

- 484 5. Djoko KY, Ong CL, Walker MJ, McEwan AG. 2015. The Role of Copper and Zinc
 485 Toxicity in Innate Immune Defense against Bacterial Pathogens. J Biol Chem
 486 290:18954-61.
- 487 6. White C, Lee J, Kambe T, Fritsche K, Petris MJ. 2009. A role for the ATP7A
- 488 copper-transporting ATPase in macrophage bactericidal activity. J Biol Chem489 284:33949-56.
- 490 7. Achard Maud ES, Stafford Sian L, Bokil Nilesh J, Chartres J, Bernhardt Paul V,

491 Schembri Mark A, Sweet Matthew J, McEwan Alastair G. 2012. Copper

- 492 redistribution in murine macrophages in response to *Salmonella* infection.
- 493 Biochem J 444:51-57.
- 494 8. Ladomersky E, Khan A, Shanbhag V, Cavet JS, Chan J, Weisman GA, Petris
- 495 MJ. 2017. Host and Pathogen Copper-Transporting P-Type ATPases Function
- 496 Antagonistically during *Salmonella* Infection. Infect Immun 85.

497	9.	Johnson MD, Kehl-Fie TE, Klein R, Kelly J, Burnham C, Mann B, Rosch JW.
498		2015. Role of copper efflux in pneumococcal pathogenesis and resistance to
499		macrophage-mediated immune clearance. Infect Immun 83:1684-94.
500	10.	Giachino A, Waldron KJ. 2020. Copper tolerance in bacteria requires the
501		activation of multiple accessory pathways. Mol Microbiol 114:377-390.
502	11.	Rensing C, Fan B, Sharma R, Mitra B, Rosen BP. 2000. CopA: An Escherichia
503		coli Cu(I)-translocating P-type ATPase. Proc Natl Acad Sci U S A 97:652-6.
504	12.	Djoko KY, Franiek JA, Edwards JL, Falsetta ML, Kidd SP, Potter AJ, Chen NH,
505		Apicella MA, Jennings MP, McEwan AG. 2012. Phenotypic characterization of a
506		copA mutant of Neisseria gonorrhoeae identifies a link between copper and
507		nitrosative stress. Infect Immun 80:1065-71.
508	13.	Solioz M, Stoyanov JV. 2003. Copper homeostasis in Enterococcus hirae. FEMS
509		Microbiol Rev 27:183-95.
510	14.	Johnson MD, Kehl-Fie TE, Rosch JW. 2015. Copper intoxication inhibits aerobic
511		nucleotide synthesis in Streptococcus pneumoniae. Metallomics 7:786-94.
512	15.	Stewart LJ, Ong CY, Zhang MM, Brouwer S, McIntyre L, Davies MR, Walker MJ,
513		McEwan AG, Waldron KJ, Djoko KY. 2020. Role of Glutathione in Buffering
514		Excess Intracellular Copper in Streptococcus pyogenes. mBio 11.
515	16.	Shafeeq S, Yesilkaya H, Kloosterman TG, Narayanan G, Wandel M, Andrew
516		PW, Kuipers OP, Morrissey JA. 2011. The cop operon is required for copper
517		homeostasis and contributes to virulence in Streptococcus pneumoniae. Mol
518		Microbiol 81:1255-70.

- 519 17. Facklam R. 2002. What happened to the streptococci: overview of taxonomic and 520 nomenclature changes. Clin Microbiol Rev 15:613-30.
- 521 18. Chen SL. 2019. Genomic Insights Into the Distribution and Evolution of Group B
 522 Streptococcus. Frontiers in Microbiology 10:1447.
- 523 19. Edwards MS, Baker CJ. 2018. 119 Streptococcus agalactiae (Group B
- 524 Streptococcus), p 723-729.e1. In Long SS, Prober CG, Fischer M (ed), Principles
- and Practice of Pediatric Infectious Diseases (Fifth Edition)
- 526 doi:<u>https://doi.org/10.1016/B978-0-323-40181-4.00119-5</u>. Elsevier.
- 527 20. Lindahl G, Stalhammar-Carlemalm M, Areschoug T. 2005. Surface proteins of
- 528 *Streptococcus agalactiae* and related proteins in other bacterial pathogens. Clin 529 Microbiol Rev 18:102-27.
- 530 21. Tuomanen E, Cozens R, Tosch W, Zak O, Tomasz A. 1986. The rate of killing of
- 531 *Escherichia coli* by beta-lactam antibiotics is strictly proportional to the rate of 532 bacterial growth. J Gen Microbiol 132:1297-304.
- 533 22. Eng RH, Padberg FT, Smith SM, Tan EN, Cherubin CE. 1991. Bactericidal
- effects of antibiotics on slowly growing and nongrowing bacteria. AntimicrobAgents Chemother 35:1824-8.
- 536 23. Sanders S, Bartee D, Harrison MJ, Phillips PD, Koppisch AT, Freel Meyers CL.
- 537 2018. Growth medium-dependent antimicrobial activity of early stage MEP
 538 pathway inhibitors. PLoS ONE 13:e0197638.
- 539 24. Peterson LR, Gerding DN, Hall WH, Schierl EA. 1978. Medium-dependent
- 540 variation in bactericidal activity of antibiotics against susceptible *Staphylococcus*
- 541 *aureus*. Antimicrob Agents Chemother 13:665-8.

- 542 25. Sullivan MJ, Ulett GC. 2020. Evaluation of hematogenous spread and ascending
- 543 infection in the pathogenesis of acute pyelonephritis due to group B
- 544 streptococcus in mice. Microb Pathog 138:103796.
- 545 26. Moulin P, Patron K, Cano C, Zorgani MA, Camiade E, Borezee-Durant E,
- 546 Rosenau A, Mereghetti L, Hiron A. 2016. The Adc/Lmb System Mediates Zinc
- 547 Acquisition in *Streptococcus agalactiae* and Contributes to Bacterial Growth and
- 548 Survival. J Bacteriol 198:3265-3277.
- 549 27. Sullivan MJ, Ulett GC. 2018. Stable Expression of Modified Green Fluorescent
- 550 Protein in Group B Streptococci To Enable Visualization in Experimental
- 551 Systems. Appl Environ Microbiol 84.
- 552 28. Ipe DS, Ben Zakour NL, Sullivan MJ, Beatson SA, Ulett KB, Benjamin WHJ,
- 553 Davies MR, Dando SJ, King NP, Cripps AW, Schembri MA, Dougan G, Ulett GC.
- 554 2015. Discovery and Characterization of Human-Urine Utilization by
- 555 Asymptomatic-Bacteriuria-Causing *Streptococcus agalactiae*. Infect Immun
- 556 84:307-19.
- 557 29. Sullivan MJ, Leclercq SY, Ipe DS, Carey AJ, Smith JP, Voller N, Cripps AW, Ulett
- 558 GC. 2017. Effect of the *Streptococcus agalactiae* Virulence Regulator CovR on
- the Pathogenesis of Urinary Tract Infection. J Infect Dis 215:475-483.
- 560 30. Untergasser A, Cutcutache I, Koressaar T, Ye J, Faircloth BC, Remm M, Rozen
- 561 SG. 2012. Primer3--new capabilities and interfaces. Nucleic Acids Res 40:e115.
- 562 31. Untergasser A, Nijveen H, Rao X, Bisseling T, Geurts R, Leunissen JA. 2007.
- 563 Primer3Plus, an enhanced web interface to Primer3. Nucleic Acids Res 35:W71-
- 564

4.

565	32.	Bustin SA, Benes V, Garson JA, Hellemans J, Huggett J, Kubista M, Mueller R,
566		Nolan T, Pfaffl MW, Shipley GL, Vandesompele J, Wittwer CT. 2009. The MIQE
567		guidelines: minimum information for publication of quantitative real-time PCR
568		experiments. Clin Chem 55:611-22.
569	33.	Sullivan MJ, Forde BM, Prince DW, Ipe DS, Ben Zakour NL, Davies MR, Dougan
570		G, Beatson SA, Ulett GC. 2017. Complete Genome Sequence of Serotype III
571		Streptococcus agalactiae Sequence Type 17 Strain 874391. Genome
572		Announcements 5.
573	34.	Pfaffl MW. 2001. A new mathematical model for relative quantification in real-
574		time RT-PCR. Nucleic Acids Res 29:e45.
575	35.	Eijkelkamp BA, Morey JR, Ween MP, Ong CL, McEwan AG, Paton JC, McDevitt
576		CA. 2014. Extracellular zinc competitively inhibits manganese uptake and
577		compromises oxidative stress management in Streptococcus pneumoniae. PLoS
578		ONE 9:e89427.
579	36.	Anders S, Pyl PT, Huber W. 2015. HTSeqa Python framework to work with
580		high-throughput sequencing data. Bioinformatics 31:166-9.
581	37.	Love MI, Huber W, Anders S. 2014. Moderated estimation of fold change and
582		dispersion for RNA-seq data with DESeq2. Genome Biol 15:550.
583	38.	Acharya D, Sullivan MJ, Duell BL, Goh KGK, Katupitiya L, Gosling D, Chamoun
584		MN, Kakkanat A, Chattopadhyay D, Crowley M, Crossman DK, Schembri MA,
585		Ulett GC. 2019. Rapid Bladder Interleukin-10 Synthesis in Response to
586		Uropathogenic Escherichia coli Is Part of a Defense Strategy Triggered by the
587		Major Bacterial Flagellar Filament FliC and Contingent on TLR5. mSphere 4.

- 588 39. Leclercq SY, Sullivan MJ, Ipe DS, Smith JP, Cripps AW, Ulett GC. 2016.
- 589 Pathogenesis of *Streptococcus* urinary tract infection depends on bacterial strain
- and beta-hemolysin/cytolysin that mediates cytotoxicity, cytokine synthesis,
- 591 inflammation and virulence. Scientific Reports 6:29000.
- 592 40. Valdes Lopez JF, Urcuqui-Inchima S. 2018. Synergism between phorbol-12-
- 593 myristate-13-acetate and vitamin D3 in the differentiation of U937 cells to
- 594 monocytes and macrophages. Morphologie 102:205-218.
- 595 41. Cumley NJ, Smith LM, Anthony M, May RC. 2012. The CovS/CovR acid
- 596 response regulator is required for intracellular survival of group B Streptococcus
- in macrophages. Infect Immun 80:1650-61.
- 598 42. Price EE, Boyd JM. 2020. Genetic Regulation of Metal Ion Homeostasis in
 599 Staphylococcus aureus. Trends Microbiol 28:821-831.
- 43. Turner AG, Djoko KY, Ong CY, Barnett TC, Walker MJ, McEwan AG. 2019.
- 601 Group A Streptococcus co-ordinates manganese import and iron efflux in
- response to hydrogen peroxide stress. Biochem J 476:595-611.
- 44. Janulczyk R, Ricci S, Bjorck L. 2003. MtsABC is important for manganese and
- 604 iron transport, oxidative stress resistance, and virulence of *Streptococcus*
- 605 *pyogenes*. Infect Immun 71:2656-64.
- 45. Culbertson EM, Bruno VM, Cormack BP, Culotta VC. 2020. Expanded role of the
- 607 Cu-sensing transcription factor Mac1p in *Candida albicans*. Mol Microbiol
- 608 114:1006-1018.

-505 $+0.$ Onabayer 0, bader 1, maderer 0, mizaitor b, openerberg b. 2010. A	609	46.	Shabayek S, Bauer R, Mauerer S, Mizaikoff B, Spellerberg B. 2016. A
--	-----	-----	---

- 610 streptococcal NRAMP homologue is crucial for the survival of *Streptococcus*
- 611 *agalactiae* under low pH conditions. Mol Microbiol 100:589-606.
- 47. Sullivan MJ, Goh KG, Ulett GC. 2021. Cellular management of Zinc in group B
- 613 Streptococcus supports bacterial resistance against metal intoxication and
- 614 promotes disseminated infection. bioRxiv:2021.02.05.42539.
- 615 48. Hood MI, Skaar EP. 2012. Nutritional immunity: transition metals at the
 616 pathogen-host interface. Nat Rev Microbiol 10:525-37.
- 49. Ong CY, Berking O, Walker MJ, McEwan AG. 2018. New Insights into the Role
- 618 of Zinc Acquisition and Zinc Tolerance in Group A Streptococcal Infection. Infect619 Immun 86.
- 620 50. Odermatt A, Solioz M. 1995. Two trans-acting metalloregulatory proteins

621 controlling expression of the copper-ATPases of *Enterococcus hirae*. J Biol622 Chem 270:4349-54.

51. Portmann R, Poulsen KR, Wimmer R, Solioz M. 2006. CopY-like copper

624 inducible repressors are putative 'winged helix' proteins. Biometals 19:61-70.

- 625 52. Beisel WR, Pekarek RS, Wannemacher RW. 1974. The impact of infectious
- disease on trace-element metabolism of the host., p 217. In Hoekstra WG, Suttie
- 527 JW, Ganther HE, Mertz W (ed), Trace element metabolism in animals, 2
- 628 University Park Press, Baltimore, MD.
- 53. Fleming RE, Whitman IP, Gitlin JD. 1991. Induction of ceruloplasmin gene
- 630 expression in rat lung during inflammation and hyperoxia. Am J Physiol 260:L68-
- 631 74.

632 54. Percival SS. 1998. Copper and immunity. Am J Clin Nutr 67:1064S-1068S. 633 Achard ME, Tree JJ, Holden JA, Simpfendorfer KR, Wijburg OL, Strugnell RA, 55. 634 Schembri MA, Sweet MJ, Jennings MP, McEwan AG. 2010. The multi-copper-ion 635 oxidase CueO of Salmonella enterica serovar Typhimurium is required for 636 systemic virulence. Infect Immun 78:2312-9. 637 56. Francis MS, Thomas CJ. 1997. Mutants in the CtpA copper transporting P-type 638 ATPase reduce virulence of *Listeria monocytogenes*. Microb Pathog 22:67-78. 639 57. Schwan WR, Warrener P, Keunz E, Stover CK, Folger KR. 2005. Mutations in 640 the *cueA* gene encoding a copper homeostasis P-type ATPase reduce the 641 pathogenicity of Pseudomonas aeruginosa in mice. Int J Med Microbiol 295:237-642 42. 643 58. Carey AJ, Tan CK, Mirza S, Irving-Rodgers H, Webb RI, Lam A, Ulett GC. 2014. 644 Infection and cellular defense dynamics in a novel 17beta-estradiol murine model 645 of chronic human group B streptococcus genital tract colonization reveal a role 646 for hemolysin in persistence and neutrophil accumulation. J Immunol 192:1718-31. 647 648 59. Juttukonda LJ, Beavers WN, Unsihuay D, Kim K, Pishchany G, Horning KJ, 649 Weiss A, Al-Tameemi H, Boyd JM, Sulikowski GA, Bowman AB, Skaar EP. 2020. 650 A Small-Molecule Modulator of Metal Homeostasis in Gram-Positive Pathogens. 651 mBio 11. 652 Takahashi S, Nagano Y, Nagano N, Hayashi O, Taguchi F, Okuwaki Y. 1995. 60. 653 Role of C5a-ase in group B streptococcal resistance to opsonophagocytic killing. 654 Infect Immun 63:4764-9.

- 655 61. Neubert MJ, Dahlmann EA, Ambrose A, Johnson MDL. 2017. Copper Chaperone
- 656 CupA and Zinc Control CopY Regulation of the Pneumococcal *cop* Operon.
- mSphere 2.
- 658

Locus_	Genbank				
tag [†]	accession	Label	Annotation	FC	FDR
02565	ASZ00809.1	сорҮ	CopY/TcrY family copper transport	4.1	1.09E-12
			repressor		
02575	ASZ00811.1	copZ	carbonate dehydratase	4.0	1.02E-37
02570	ASZ00810.1	сорА	copper-translocating P-type ATPase	3.7	2.25E-35
10970	ASZ02392.1		peptidoglycan-binding protein LysM	3.4	6.13E-13
07965	ASZ01821.1	mtsA	metal ABC transporter substrate-binding	2.9	2.15E-12
			protein		
07960	ASZ01820.1	<i>mt</i> sB	metal ABC transporter ATP-binding	2.6	1.02E-15
			protein		
10190	ASZ02237.1	mntH2	divalent metal cation transporter	2.4	6.34E-09
10965	ASZ02391.1		transglycosylase	2.2	1.87E-06
09125	ASZ02032.1		CHAP domain-containing protein	2.1	1.58E-09
07955	ASZ01819.1	mtsC	metal ABC transporter permease	2.1	2.62E-10
10305	ASZ02261.1		PAP2 family protein	2.0	6.13E-13
08045	ASZ01834.1		glycosyltransferase family 2 protein	-2.0	9.51E-06
08200	ASZ01861.1		branched-chain amino acid ABC	-2.3	1.98E-04
			transporter substrate-binding protein		
10430	ASZ02284.1	hvgA	pathogenicity protein	-2.3	2.18E-07
04720	ASZ01199.1	pcl1	membrane protein	-4.3	1.38E-09
04185	ASZ01095.1	fetB	iron export ABC transporter permease	-4.9	1.39E-08
			subunit, FetB		
04180	ASZ01094.1	fetA	ABC transporter ATP-binding protein	-4.9	4.58E-11
.			FetA		

659 TABLE 1. Transcriptional signature of Cu intoxication in GBS

660

[†] denotes locus tag of *S. agalactiae* 874391, preceded by CHF17_RS

661 TABLE 2. Bacterial strains and Plasmids

Bacteria	Bacteria 662				
Strains	Characteristics	Source			
<i>E. coli</i> DH5α	huA2 lac(Δ)U169 phoA glnV44 Φ80' lacZ(Δ)M15 gyrA96 recA1 relA1 endA1 thi-1 hsdR17	Bethesda Research Labs			
S. agalactiae 874391	Wild type, Sequence type-17, Serotype III strain, Vaginal isolate (Japan)	(60)			
S. agalactiae GU2691	874391∆ <i>copA</i> (<i>copA</i> mutant) Locus tag: CHF17_RS02570	This work			
S. agalactiae GU2857	874391∆ <i>copY</i> (<i>copY</i> mutant) Locus tag: CHF17_RS02565	This work			
S. agalactiae GU3121	GU2857 (Δ <i>copA</i>) containing <i>copYAZ</i> complement construct pGU3112; Sp	This work			
Plasmids					
pHY304aad9	ori (Ts); temperature-sensitive shuttle vector; Sp	(28)			
pGU2650	pHY304 <i>aad9-</i> derivative <i>copA</i> ∆ construct; Sp	This work			
pGU2847	pHY304 <i>aad</i> 9-derivative <i>cop</i> Y∆ construct; Sp	This work			
pGU3112	pDL278 containing cloned copYAZ operon; Sp	This work			

663	FIG 1. Global transcriptomic analysis of GBS in response to Cu stress. Volcano plot
664	showing data from RNASeq analysis of WT GBS cultures exposed to 0.5 mM Cu
665	compared to non-exposed controls. Transcripts detected as up- or down-regulated in
666	response to Cu ($n=4$, >± 2-fold, FDR <0.05) are highlighted in red and blue,
667	respectively. Dotted lines show False discovery rate (FDR; q-value) and fold-change
668	cut-offs. Grey points indicate genes that were not significant changed in expression,
669	according to these analysis cut-offs. Selected genes are identified with black lines. B,
670	Validation of RNASeq data. Expression ratio (Fold-change) of <i>pcl1</i> , <i>hvgA</i> and <i>copY</i>
671	quantified by qRTPCR in THB medium containing 0.5 mM Cu compared to THB without
672	Cu. Ratios for qRTPCR were normalized using housekeeping <i>dnaN</i> and RNASeq ratios
673	were calculated using DESeq2. Bars show means and S.E.M from 4 independent
674	experiments.
675	

676 FIG 2. Organisation of the copY-copA-copZ locus in GBS. A, copY-copA-copZ are 677 adjacent in the GBS genome and likely controlled by the promoter-proximal copY, 678 encoding a putative Cu-sensing repressor. Locus tags from the GBS 874391 genome 679 are indicated. B, Distribution of homologous cop genes in other Lactobacillales, 680 arranged by percentage identity of amino acid sequence to CopA of S. agalactiae. C, 681 Model of Cu efflux in GBS highlighting CopA as transmembrane Cu exporter, 682 transcriptionally repressed by CopY in the absence of Cu, which is likely inhibited by the 683 Cu-binding chaperone protein CopZ. Figure based on previous studies in other 684 lactobacillales (51, 61).

FIG 3. Growth curve analyses of GBS cultured in nutrient-rich THB medium (A), or in THB supplemented with 0.5 mM Cu (B), 1.0 mM Cu (C) or 1.5 mM Cu (D), comparing WT, $\triangle copA$ or $\triangle copY$ strains as indicated in panel A. Points and bars show mean and S.E.M of 3 independent experiments monitoring attenuance at 600nm. **FIG 4.** Bactericidal effect of Cu on GBS viability. Time-kill assays comparing WT, $\triangle copA$

or $\triangle cop Y$ GBS, incubated in CDM or in CDM supplemented with 0.05, 0.1, 0.2, 0.5 or 1 mM Cu. Viable cells were quantified at 1h, 3h, 6h and 24h post inoculation. [†] Viable Cell counts of 0 CFU/mL were assigned a value of 1 to enable visualisation on log₁₀ y-axes. Points and bars show mean and S.E.M of 4 independent experiments. Data were analysed by One-way ANOVA with Holm Sidak Multiple comparisons, comparing Cuexposed conditions to non-exposed controls (0 mM Cu) at each time-point, for each

697 strain (* P < 0.05, ** P < 0.01. *** P <0.001).

698

699 **FIG 5.** Expression analysis of *copA* and intracellular Cu content in GBS strains. A. 700 Expression ratio (Fold-change) of *copA* quantified by qRT-PCR in THB medium 701 containing 0.25, 0.5, 1.0 and 1.5 mM Cu, compared to THB without Cu. B, Relative 702 copA transcripts were quantified in WT and $\triangle copY$ strains with and without Cu 703 supplementation (0.5 mM) to demonstrate de-regulation of *copA* expression in the 704 $\Delta cop Y$ background. C, Final biomass yield comparisons of WT, $\Delta cop A$ and $\Delta cop Y$ 705 strains following growth for 18h in THB with 1.5 mM Cu. D, Intracellular accumulation of 706 Cu was compared with and without Cu supplementation (0.5 mM) in WT, $\triangle copA$ and 707 $\Delta cop Y$ strains. Ratios in A were calculated as described previously (34) using C_T

values, primer efficiencies and housekeeping *dnaN*. Bars show means and S.E.M from
3-4 independent experiments and compared by One-way ANOVA with Holm-Sidak
multiple comparisons (*** P <0.001).

711

FIG 6. Interactions of GBS with macrophages of mouse and human origin. Gentamicin protection assays with WT and $\triangle copA$ strains and mouse (J774A.1) or human (U937 monocyte-derived macrophage-like) macrophages. Surviving bacteria are expressed as rCFU, indicating the difference between the number of initial intracellular bacteria (1h after antibiotic treatment) and the number of intracellular bacteria at 24h or 48h post infection (h.p.i). Data are means and S.E.M of 4-5 independent experiments.

FIG 7. Virulence of WT (grey circles) or $\triangle copA$ (blue diamonds) GBS (orange triangles)

in a mouse model of disseminated infection. C57BL/6 mice (6-8 weeks old) were

721 intravenously injected with 10^7 bacteria; bacteremia and disseminated spread to liver

and spleen were monitored at 24h post infection. CFU were enumerated and counts

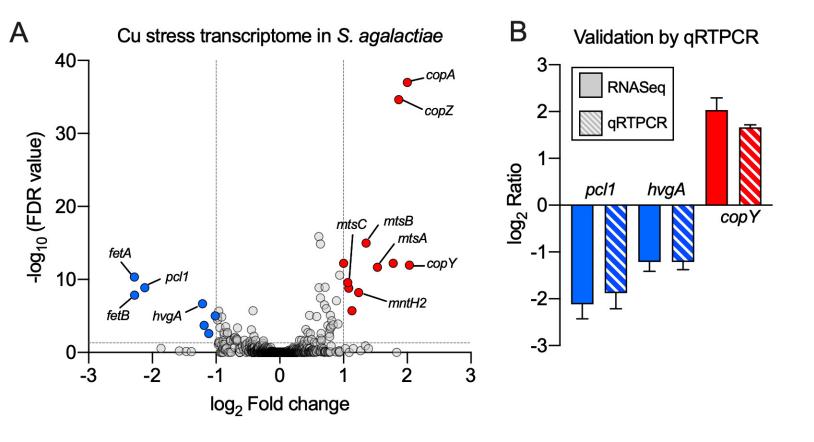
723 were normalized using tissue mass in g. Lines and bars show median and interquartile

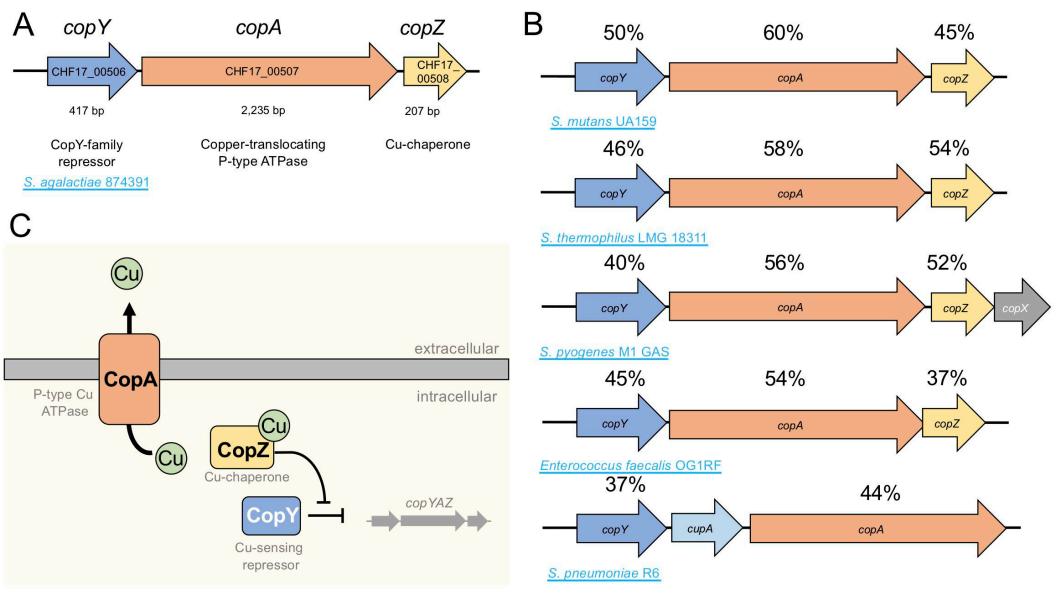
ranges and data are pooled from 2 independent experiments each containing n=10

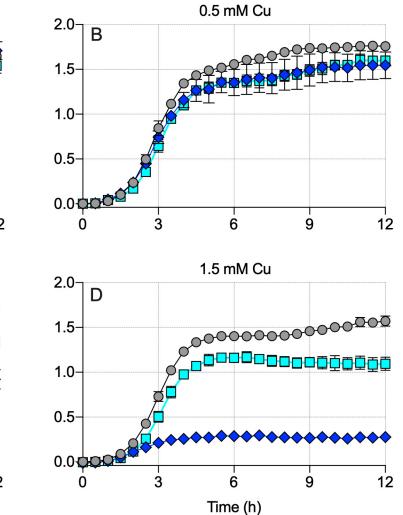
mice compared using Mann-Whitney U-tests (*P < 0.05, **P < 0.01).

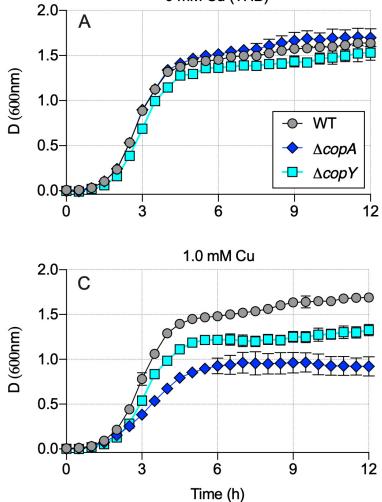
726

Supplementary FIG S1. Complementation of *copA* mutation restores growth of GBS to WT levels under Cu stress. Growth curve analyses of GBS cultured in nutrient-rich THB medium (A), or in THB supplemented with 0.5 mM Cu (B), 1.0 mM Cu (C) or 1.5 mM Cu (D), comparing WT, $\triangle copA::copA$ strains.









0 mM Cu (THB)

